

Computational method for researching turbulent velocity head in wind tunnel

Oleksander Zhdanov^{1,†}, Victor Dehtiarov^{1,†} and Olha Sushchenko^{1,*,†}

¹State University "Kyiv Aviation Institute", Liubomyra Huzara Ave., 1, Kyiv, 03058, Ukraine

Abstract

This paper deals with researching the turbulent velocity head in the wind tunnel. The new equipment to reduce labor and energy costs for measurements and information assessment in the system mentioned above is proposed. A detailed description of the appropriate equipment is given. The usage of the one-degree-of-freedom coordinate unit is grounded. The design features of the comb with pressure sensors are represented. The algorithm for the information and measuring system operation has been developed. The basic stages of the computational method are described. The program realization of the technique in LabVIEW is characterized. The appropriate graphical dependencies, which represent the results of the developed method, are given.

Keywords

computational method, information and measurement system, turbulent velocity head, wind tunnel, experimental equipment

1. Introduction

The problems of researching the aerodynamic characteristics of aircraft in wind tunnels have a definite history [1]. Research on vortex generators in the turbulent flow is described in [2]. The influence of edge protuberances on the aircraft's wing characteristics is represented in [3, 4]. Studies of the aircraft characteristics in the wind tunnel have been given in [5, 6]. The features of tools in experiments in the wind tunnel are represented in [7]. The first studies of the influence of volumetric vortex generators installed on the nose of the aircraft airfoil began in the Aerodynamic Research Laboratory at the Department of Aerodynamics and Flight Safety of the Kyiv Aviation Institute back in 2006 under the leadership of Doctor of Technical Sciences, Prof. E.P. Udartsev [8]. The first patents on volumetric vortex generators date back to 2010 [9, 10]. In 2018–2025, a large amount of experimental research was carried out in the wind tunnel of the laboratory on the influence of installing volumetric vortex generators on the aerodynamic characteristics of airfoil models of various types. Volumetric vortex generator kits for installation on blowing models were designed and manufactured on a 3-D printer. Studies have shown the effectiveness of using volumetric vortex generators to improve the change in aerodynamic characteristics in the critical and subcritical areas of angles of attack, and the possibility of maintaining and improving the flight characteristics in cruising flight modes [11, 12]. The research mentioned above can be used in the synthesis of control laws for aircraft of various types [13, 14]. This improves the safety of flights [15, 16, 17, 18].

Due to the increased requirements for the development and operation of highly manoeuvrable and all-weather unmanned aerial vehicles, the above-mentioned topic has become particularly relevant today. The computational method of researching turbulent head velocity represents a direct continuation of the previous research. It is aimed to improve the flight and technical characteristics of aircraft in terms of increasing flight safety in conditions of wind gusts, piloting errors by expanding the operational limits of angles of attack and sideslip beyond critical values. The proposed approach improves characteristics stability and controllability and ensures acceptable aerodynamic quality in cruising flight modes.

CMSE'25: International Workshop on Computational Methods in Systems Engineering, June 12, 2025, Kyiv, Ukraine

*Corresponding author.

†These authors contributed equally.

✉ azhdanov@kai.edu.ua (O. Zhdanov); vitdeg50@gmail.com (V. Dehtiarov); sushoa@ukr.net (O. Sushchenko)

ORCID 0000-0001-5273-571X (O. Zhdanov); 0000-0000-0000-0000 (V. Dehtiarov); 0000-0002-8837-1521 (O. Sushchenko)



© 2025 Copyright for this paper by its authors. Use permitted under Creative Commons License Attribution 4.0 International (CC BY 4.0).

A lot of work has been done to renew and adjust the experimental equipment to realize the proposed computational method. In particular, this concerned the wind tunnel, on which the multi-fan installation was modernized by replacing all 12 metal blades of imperfect aerodynamic shape on all 12 fans with specially designed and manufactured aerodynamically high-quality plastic ones for specific dimensions of the fan flow part and operating speeds, for right and left directions of rotation. The blades have a geometric twist along the length, a variable chord, and curvature of the profile. The modernization increased the efficiency of the wind tunnel; the airflow velocity in the empty working part of the wind tunnel increased by $\approx 18\%$.

2. Description of information and measurement system

The basic approaches to implementing tests in the wind tunnel are given in [19, 20, 21].

The study of the airflow velocity field requires the creation of new equipment to reduce labor and energy costs for measurements and information assessment. The vertically moving rod with an air pressure receiver at the end is a part of the equipment used in the research. Usually, the rod is moved and fixed at the desired point by the operator in the Eiffel chamber above the working part of the wind tunnel.

Initially, the possibility of installing an electromechanical drive for vertical movement of the rod was considered. The main feature of this approach is the use of the one-degree-of-freedom coordinate unit with a movement control system and computer-realized measurements. The drive mechanism of the coordinate unit is located on the construction elements of the ceiling outside the working part in specific places. The choice of these places is defined by the possibility of pushing out a rod with an air pressure receiver above the ceiling of the working part. In this case, the function of manual movement of the air pressure receiver and the presence of the researcher in the Eiffel chamber are eliminated.

Implementing the idea of a three-degree-of-freedom coordinate unit, or at least a two-degree-of-freedom coordinate unit, involves creating a complex structure of guides and mechanisms for moving in the direction of three coordinate axes. These guides and mechanisms must be mounted in the working part. Thus, they can create considerable clutter and difficulties for the measuring process. This can negatively influence measurement results. At the same time, labour and energy costs will decrease insignificantly.

In this paper, a new idea is proposed. It lies in applying a comb with nine air pressure receivers instead of one. The comb is installed vertically in the desired location and is fixed with one end to the floor and the other to the ceiling of the working part of the wind tunnel. The realization of this idea provides simultaneous measurement of airflow parameters at nine points located vertically for a given flow velocity. After measurements, wind tunnel fans are turned off, the comb is moved to a new location, and the test continues.

Structurally, the comb represents a rectangular cross-section steel rod on which nine tubular air pressure receivers and sets of appropriate serving units are mounted. Connections represent a system of electrical and pneumatic lines. After calibrating pressure sensors installed on the comb, it is necessary to renew the communication of pneumatic lines serving the set of sensors of single-barrel air pressure receivers. These operations provide the working state of the equipment required for experimenting. The measuring system is completed by a surface unit. Therefore, the comb can be installed in the desired place of the working part of the wind tunnel. Examples of the location of the combs in the working part are shown in Fig. 1 In the lower part of the comb, you can see the output of two cables with power and information wires for two lines of pressure sensors. The cables connect the comb sensors to the computer located in the operator room. A pneumatic line tube comes out, which supplies atmospheric pressure from the operator's room as a reference to the pressure sensors serving the six-barrel air pressure receiver.

The design features of the comb are the location of pressure sensors close to the inlets of the air pressure receiver tubes. The short length of the pneumatic lines, $\sim 15 \div 20$ cm, allows us to study air pressure fluctuations as a characteristic of the turbulence in a wide frequency range compared to the

pneumatic line, ~ 12 m long, which is used during flow velocity measurements in research experiments.



Figure 1: The comb in the working part of the wind tunnel (at the section of the nozzle and inside the wind tunnel).

The information and measuring system provides measurement of the following airflow parameters in the working part of the wind tunnel: full pressure P_f ; static pressure P_{st} , coefficient of air pressure receiver ξ_{apr} ; density of air ρ ; airflow velocity V .

The algorithm of the information and measuring system can be described as follows. The first group of sensors is installed inside the comb. It includes eight air pressure receivers and eight pressure sensors (measuring channels 0-7). They measure the pressure difference between the total and static pressures

$$\Delta P_i = P_{if} - P_{ist}. \quad (1)$$

Next, the velocity head

$$q_i = \xi_{iapr} \Delta P_i, \quad (2)$$

the airflow velocity

$$V_i = \sqrt{2q_i/\rho}, \quad (3)$$

the average velocity head

$$q_{iav} = \sum_{i=1}^N \frac{q_i}{N}, \quad (4)$$

the average speed

$$V_{iav} = \sum_{i=1}^N \frac{V_i}{N}, \quad (5)$$

and the turbulence degree

$$\varepsilon = \frac{\sqrt{\sum_{i=1}^N (V_i - V_{iav})^2 / N}}{V_{iav}}, \quad (6)$$

are determined, where N is the number of measurements in the sample.

Formulas (1) – (6) allow us to determine basic parameters of the velocity head. The calculation of measuring results has been realized by techniques represented in [22, 23]. Averaging of measuring results has been implemented according to the expressions given in [24].

The coefficients of the airflow velocity head at the location of the air pressure receivers are determined in the following way

$$\mu_{q_i} = q_{iav} / \Delta P_{ecav}. \quad (7)$$

In formula (7), it is necessary to use the pressure drop in the Eiffel chamber P_{ec} relative to the atmospheric pressure P_{atm}

$$\Delta P_{ecav} = \sum_{i=1}^N (P_{ec} - P_{atm}). \quad (8)$$

Values (8) are determined using computer calculations based on the average values of the sensor readings.

Based on (7), the air velocity coefficients μ_V , become

$$\mu_{V_i} = \sqrt{\mu_{q_i}}. \quad (9)$$

If the airflow velocity V_i is not calculated, then it is possible to determine

$$V_{iav} = \sqrt{2q_{iav} / \rho}. \quad (10)$$

However, the formula (10) does not allow us to determine the degree of turbulence.

The calculation of coefficients by expressions (7) and (9) requires applying the special equipment and a calibration technique.

The second group of sensors is also installed inside the comb and contains 6 sensors that serve 6 barrel nozzles (measuring channels 8–13). Sensors 91, 93, and 94, 95 measure pressure drops in the side channels of the air pressure receiver nozzle relative to atmospheric pressure. They are used to determine the directions of the airflow in the vertical and horizontal planes of the working part of the air duct. The layout of the holes on the air pressure receiver nozzle is shown in Fig. 2.

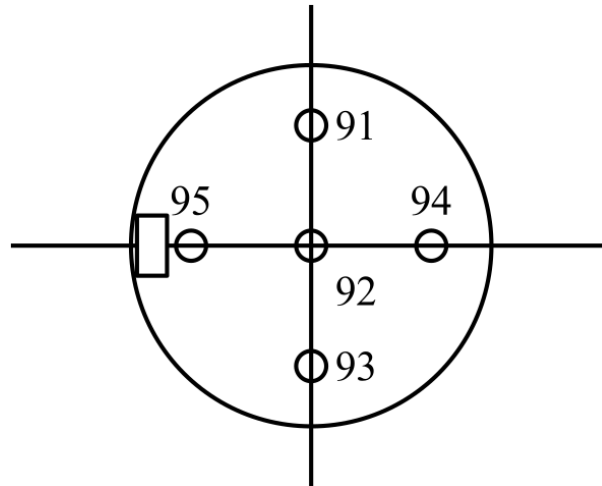


Figure 2: The location and numbering of receiving holes of the six-barrel air pressure receiver.

During the experiment, the average values of pressure drops on sensors 91, 93, and 94, 95 (see Fig. 2) are determined and recorded. In the formulas, you can use the average values of pressure drops for a certain time interval (or in each measurement cycle), define the instantaneous pressure differences between the sensors by the expressions, and then determine the average values of ΔP_{1av} , ΔP_{2av} .

$$\Delta P_{1av} = [(\Delta P_{91} - \Delta P_{92}) - (\Delta P_{93} - \Delta P_{92})] / [(\Delta P_{91} - \Delta P_{92}) - (\Delta P_{93} + \Delta P_{92})] \quad (11)$$

$$\Delta P_{2av} = [(\Delta P_{94} - \Delta P_{92}) - (\Delta P_{95} - \Delta P_{92})] / [(\Delta P_{94} - \Delta P_{92}) - (\Delta P_{95} + \Delta P_{92})] \quad (12)$$

In formulas (11) and (12), sensor 92 measures the total pressure, and sensor 96 measures the static pressure relative to atmospheric pressure. In the experiment, the average values of pressure drops are determined and recorded.

The average value of static pressure from sensor 96 is recorded and used to analyze the change in static pressure along the length of the working part of the wind tunnel. The difference in pressures of sensors 92 and 96 is determined at each sensor measuring cycle to calculate the velocity head $q_9 = \xi_{9apr}(P_{92} - P_{96})$ and the remaining flow parameters in the same way as for the air pressure receivers of the first group.

3. Computational method of determining characteristics of turbulent velocity head in wind tunnel

The computational method for researching turbulent velocity head in the wind tunnel was developed to determine the velocity head coefficients μ_q using special experimental equipment with calibrated air pressure receivers simultaneously at nine points located one above the other with a fixed step.

The velocity field of the airflow in the working part of the wind tunnel was studied in five sections with coordinates (distance from the nozzle cut towards the fans) $X_1 = 0 \text{ mm}$, $X_2 = 1130 \text{ mm}$, $X_3 = 1990 \text{ mm}$, $X_4 = 3030 \text{ mm}$, $X_5 = 4000 \text{ mm}$. In this case, the values of the velocity head coefficients μ_q were determined simultaneously for nine heights of the working part of the wind tunnel with coordinates $Y = -1000 \text{ mm}$, -700 mm , -450 mm , -200 mm , 0 mm , 200 mm , 450 mm , 700 mm , 1000 mm .

Determining the velocity head coefficients μ_q was performed by measuring the signals (pressure drops) on the air pressure receivers using an information and measuring system consisting of 15 pressure sensors of the MPXV-5004 type manufactured by Freescale Semiconductor, connected by pneumatic lines (tubes up to 0.2 m long) to 9 air pressure receivers.

In addition to calculating the velocity head coefficients of the airflow in the wind tunnel, the pressure drop in the Eiffel chamber ΔP_{ec} is measured. The electrical signal from the pressure sensors is fed to the input of a multi-channel analog-digital converter of the PCI-1746U type manufactured by Advantech, and then to a computer. The above-described structural scheme of the information and measuring system is shown in Fig. 3.

The computer realization of the information and measuring system has been implemented in the environment of the specialized graphical programming tool LabVIEW, developed by National Instruments (USA) [25, 26, 27].

The user interface of the program for researching is shown in Fig. 4.

The computational method for the research of the turbulent velocity head in the wind tunnel includes several stages:

- Preparation for setting up components of the information and measuring system.
- Setting the current parameters of the experiment.
- Monitoring the signals and performing corrections of the current values of the measuring voltage and velocities.
- Carrying out the experiment, estimating and recording the measurement results.

At the preparatory stage, the dynamic pressure conversion coefficients of all air pressure receivers and their height coordinates are entered into the program. You can check the correctness of the entered data on the indicators when the program is running. In this case, it is necessary to take into account the binding of vertical coordinates to the middle of the tunnel; the displacement of values is approximately 1.25 m.

The initial data include meteorological conditions of the experiment: temperature, humidity, and atmospheric pressure. These parameters are used to calculate the air density outside and inside the wind tunnel (in the Eiffel chamber).

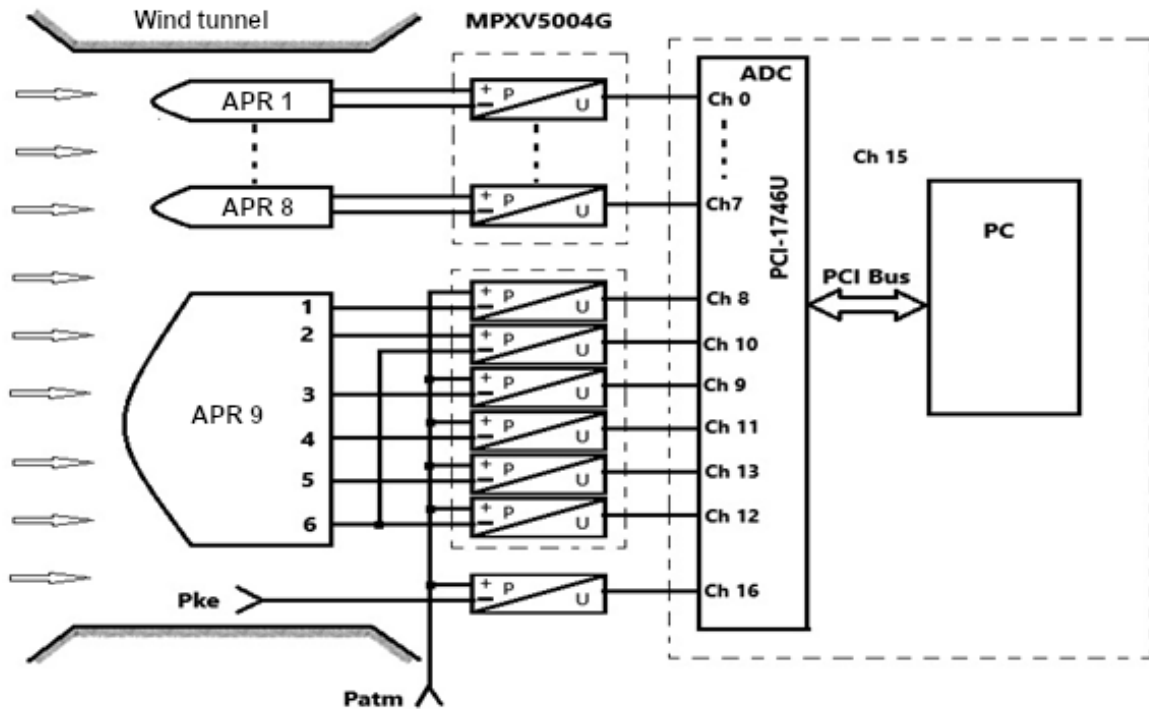


Figure 3: The structural scheme of the information and measuring system for the research head velocity field in the wind tunnel: APR is an air pressure receiver; ADC is an analog-digital converter; PC is a personal computer.

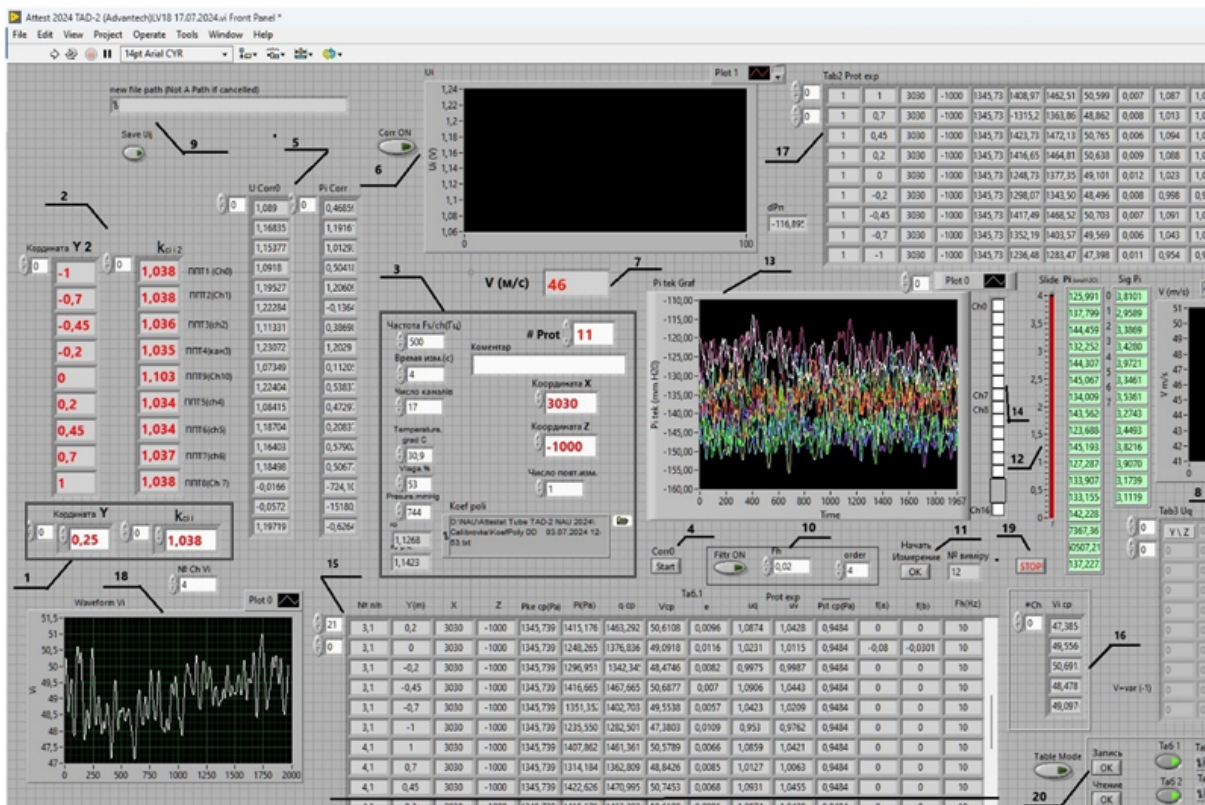


Figure 4: The user interface.

The initial data also includes the parameters of the measurement signal sampling, such as the sampling frequency and the duration (measurement time). The number of measuring channels is 17 (two groups

of 8 pressure sensors, one additional one in the Eiffel chamber, and two sensors are free).

During the experiment, it is desired to repeat measurements to improve the reliability and accuracy of the results. The calculation of the airflow velocity using air pressure receivers and sensors requires entering the conversion coefficients, taking into consideration the calibration procedure.

Before starting the experiment, to reduce the influence of noise on the measurement results, the upper limit of the digital filters of the signals coming from the pressure sensors should be chosen. The bandwidth frequency is set in relative units from the sampling frequency.

During the experiment, a series of measurements is performed for different positions of the air pressure receivers in the wind tunnel cross-section. It is possible to record time signals of pressure sensors, for example, for their further digital processing (spectral, correlation, statistical characteristics).

After starting the wind tunnel and setting the required airflow velocity, the measurement process is started. At the beginning of the first measurement, the path for storing the file of time realizations of pressure sensor signals is prescribed. A standard window for searching and selecting the definite file on the internal disk automatically appears. The file name is also automatically formed and displayed in the window. During repeated measurements, new time realizations are added to the already created file.

Next, the air pressure receiver's pressure sensors are cyclically polled, and the values of pressures and speeds, and other parameters are calculated.

Measurement results can be observed using indicators that perform the following functions:

- Accompany the measurement process and show the time of its completion.
- Display the realizations of air pressure signals, and it is possible to consider the realizations of individual channels in more detail.
- Show the average values of the realizations of the air pressures and their root mean square values.
- Show the realizations of the velocity signals.

The main results are presented as a data array. For more convenient analysis, the data can be grouped by the height of the air pressure receivers.

At the end of the measurement series, the results are saved.

The program for studying the velocity field in the wind tunnel, realized in LabVIEW, is represented in Fig. 5.

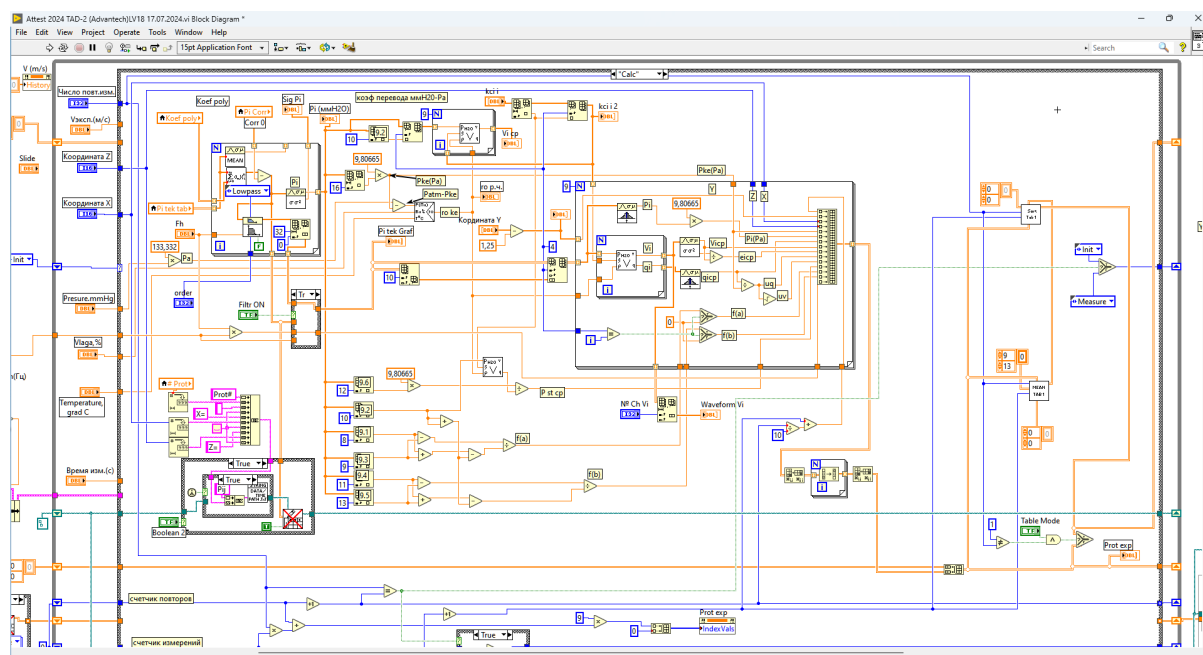


Figure 5: The fragment of the program implemented in LabVIEW.

As a result of the research, eight air pressure receivers and three receivers of a known design were tested. Since measuring the airflow velocity field in the working part of the wind tunnel was carried out by air pressure receivers installed in a special structure (fairing), a similar structure was used during calibration. In addition, some air pressure receivers were studied in isolation on a rod holder. The obtained results, in combination with improved inertial sensors, can be useful in aircraft of increased reliability [28, 29].

4. Results of the application of the computational method of determining turbulent head velocity

The main individual parameter required for air pressure receivers is the dynamic pressure conversion coefficient K_t , which was determined experimentally for each air pressure receiver in the wind tunnel.

To calibrate air pressure receivers and determine their K_t , a special software in the LabVIEW graphical programming tool was developed [25, 26].

To determine the repeatability of the research results, separate air pressure readings were used. All air pressure receivers were tested in the maximum possible speed range. Figure 6 shows a graph of the dependence of the dynamic pressure conversion coefficient K_t on the airflow velocity V for one air pressure receiver for the full test range.

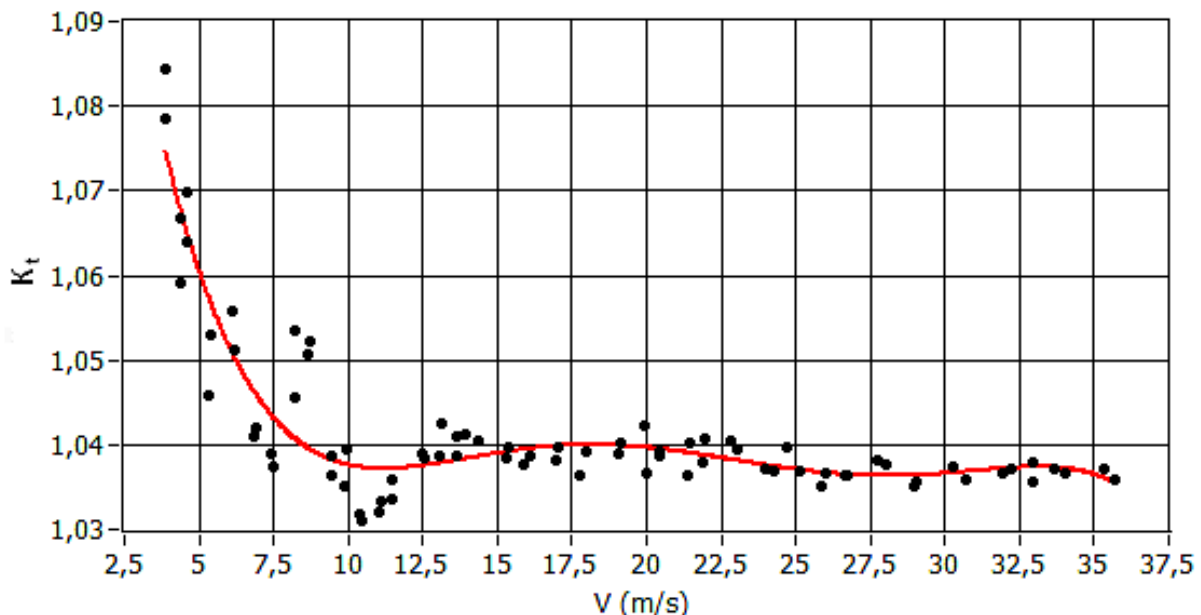


Figure 6: The dependence of the coefficient of conversion of dynamic pressure.

From the above graph, it is clear that, starting from a speed of 12 m/s, the dependence is practically linear.

The spectra of velocity signals for different average values of average V , depending on the number of fans N included in the wind tunnel, are represented in Figures 7 and 8. These graphs also show the values of the turbulence coefficients at a height of 0.7 m along the wind tunnel.

The signal spectrum at the output of pressure sensors or the airflow velocity signal can be divided into two zones: one contains components from 0 to 20 Hz, caused by airflow fluctuations (flow component), and the noise in the range of 20 Hz. The physical foundations (properties) of the origin of the flow component and noise allow us to conclude that their frequency characteristics are different.

The flow component signal is lower-frequency and does not exceed several tens of hertz (Fig.8). The flow component is due to the instability of the airflow dispersion system (fans), aerodynamic effects in the channels of the wind tunnel, which has a large size and represents a system with high inertia.

The noise is caused by the airflow passing along the small holes of the air pressure receivers and leads to the emergence of local aerodynamic effects [30, 31]. This is realized in the form of "whistling", "rustling", collapse, etc. The noise signal is higher-frequency and, as can be seen from Fig. 7, is uniform.

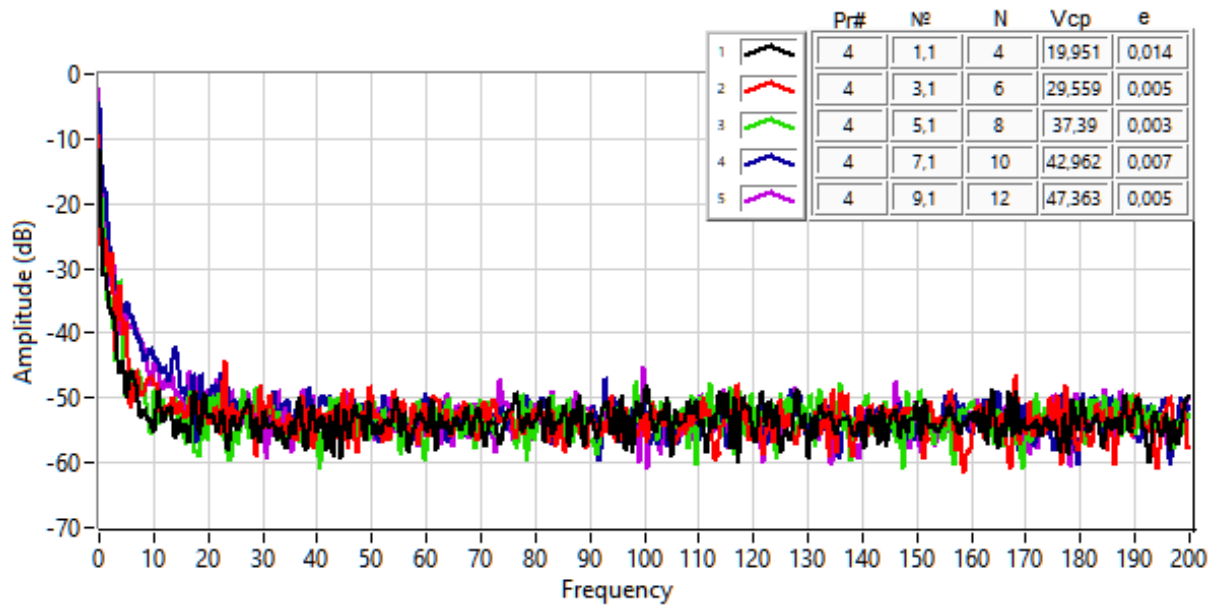


Figure 7: Signal spectrum of instantaneous airflow velocity values in the wind tunnel in a range up to 200 Hz.

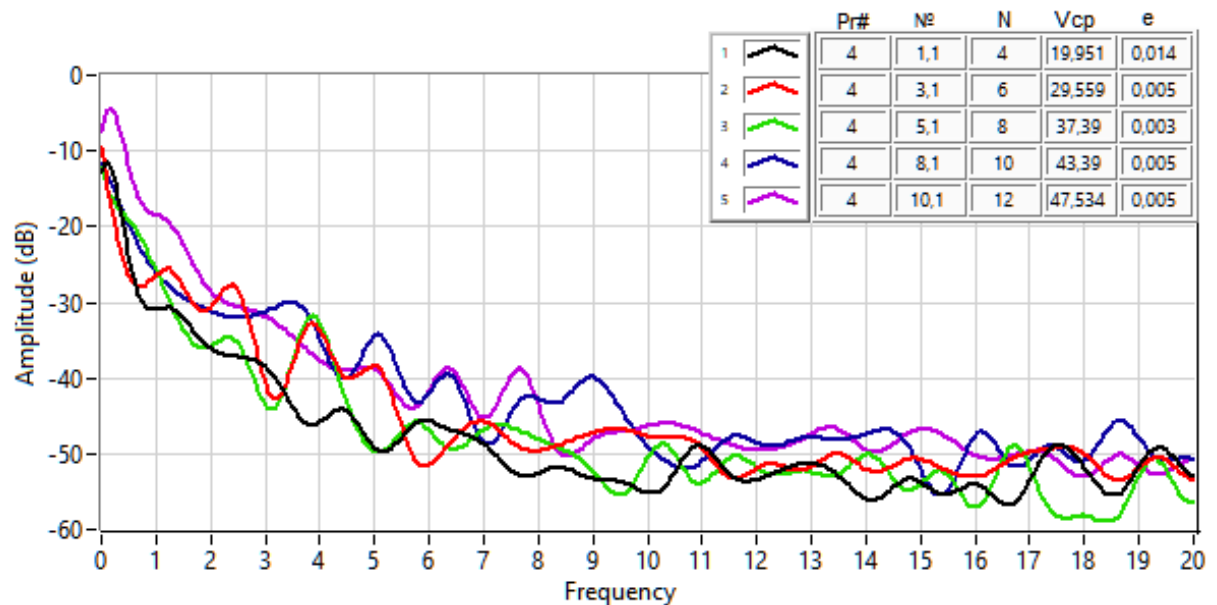


Figure 8: Signal spectrum of instantaneous airflow velocity values in the wind tunnel in a range up to 20 Hz.

Although the level of the noise spectral components is much lower than the level of the flow component of the spectrum, the influence of the noise component on the level of the root-mean-square deviation can be significant, given the increased width of the range of noise components (from 10 to 250 Hz). Therefore, when measuring the degree of turbulence of the airflow, it is desirable to take into account only the flow component of the pressure sensor signal and exclude the noise component.

The proposed technique, together with the robust approach to the stabilization laws, can ensure the high precision of stabilization processes [32, 33, 34]. The obtained results can also be useful for other engineering applications [35, 36, 37].

5. Conclusions

A detailed analysis of the experimental equipment necessary for determining the turbulent velocity head has been done.

Features of mounting air pressure receivers are described. The structural scheme of the information and measurement system and the algorithm of its operation are represented.

The basic stages of the computational method for determining the turbulent head velocity are given. The descriptions of preparatory setting components of the information and measuring system, setting the current parameters of the experiment, monitoring the signals, correcting the current values of measuring signals, carrying out the experiment, estimating and recording the measurement results are represented.

The program realization of the computational method in the LabVIEW system has been developed.

The results of applying the computational method for determining the turbulent velocity head are given.

The dependence of the dynamic pressure conversion coefficient K_t on the airflow velocity V for one air pressure receiver for the full time range is represented.

The signal spectra of instantaneous airflow velocity values in the wind tunnel in the ranges up to 200 Hz and 20 Hz are shown.

The represented research is important for improving aircraft operating efficiency in difficult conditions of external disturbances and complex manoeuvres.

The future work foresees the description of the calibration technique necessary for the efficient operation of air pressure receivers.

Acknowledgments

This research is supported by the Ministry of Education and Science of Ukraine under the project “Grounding aerodynamic layouts of promising unmanned aerial vehicles with volumetric vortex generators on aerodynamic surfaces” (# 0124U000221).

Declaration on Generative AI

The author(s) have not employed any Generative AI tools.

References

- [1] C. J. Lin, Review of research on low-profile vortex generators to control boundary-layer separation, *Progress in Aerospace Sciences* 38 (2002) 389–420. doi:10.1016/S0376-0421(02)00010-6.
- [2] J. S. Delinero, J. M. D. Leo, M. E. Camocardi, Vortex generators effect on low reynolds number airfoils in turbulent flow, *International Journal of Aerodynamics* 2 (2020) 1–14. doi:10.1504/IJAD.2012.046539.
- [3] H. Johari, C. Henocho, D. Custodio, A. Levshin, Effects of leading-edge protuberances on airfoil performance, *AIAA Journal* 45 (2007) 2634–2642. doi:10.2514/1.28497.
- [4] A. K. Malipeddi, N. Mahmoudnejad, K. A. Hoffmann, Numerical analysis of effects of leading-edge protuberances on aircraft wing performance, *Journal of Aircraft* 49 (2012) 1336–1344. doi:10.2514/1.C031670.
- [5] D. Custodio, C. W. Henocho, H. Johari, Aerodynamic characteristics of finite span wings with leading-edge protuberances, *AIAA Journal* 53 (2015) 1878–1893. doi:10.2514/1.J053568.
- [6] P. S. Divekar, T. Ekbote, Design of aerodynamic of an airplane wings, *International Journal of Scientific Development and Research (IJS DR)* 4 (2019) 59–64. URL: <https://www.ijedr.org/viewpaperforall.php?paper=IJS DR1910011>.

- [7] K. A. Salem, G. Palaia, C. Vittorio, B. Vincenzo, Tools and methodologies for box-wing aircraft conceptual aerodynamic design and aeromechanic analysis, *Mechanics and Industry* 22 (2021) 1–19. doi:10.1051/meca/2021037.
- [8] E. P. Udartsev, S. I. Alekseenko, O. I. Zhdanov, Unsteady aerodynamics of a vortex jet wing of an unmanned aerial vehicle at large and closed angles of attack, *Electronics and Control Systems* 4 (2015) 40–45. URL: http://nbuv.gov.ua/UJRN/etsu_2015_4_8.
- [9] E. P. Udartsev, O. I. Zhdanov, O. I. Shcherbonos, Generator of vortices, 2010. Patent of Ukraine. UA49403, 26.04.2010.
- [10] O. I. Zhdanov, et al., Windmill blade, 2010. Patent on the useful model. UA 49404 U, Bulletin No. 21.
- [11] O. Zhdanov, V. Orlianskyi, O. Sushchenko, Researching influence of vortex generators on aircraft aerodynamic characteristics, in: *Proceedings of the 2nd International Workshop on Advances in Civil Aviation Systems Development (ACASD 2024)*, volume 992 of *Lecture Notes in Networks and Systems*, Springer, Cham, 2024, pp. 410–422. doi:10.1007/978-3-031-60196-5_30.
- [12] M. Zaliskyi, O. Solomentsev, O. Holubnychyi, I. Ostroumov, O. Sushchenko, Y. Averyanova, et al., Methodology for substantiating the infrastructure of aviation radio equipment repair centers, *CEUR Workshop Proceedings* 3732 (2024) 136–148.
- [13] O. Holubnychyi, M. Zaliskyi, I. Ostroumov, O. Sushchenko, O. Solomentsev, Y. Averyanova, et al., Self-organization technique with a norm transformation based filtering for sustainable infocommunications within cns/atm systems, in: I. Ostroumov, M. Zaliskyi (Eds.), *Proceedings of the 2nd International Workshop on Advances in Civil Aviation Systems Development. ACASD 2024. Lecture Notes in Networks and Systems*, vol. 992, Springer Nature Switzerland, Cham, 2024, pp. 262–278. doi:10.1007/978-3-031-60196-5_20.
- [14] O. Solomentsev, M. Zaliskyi, O. Holubnychyi, I. Ostroumov, O. Sushchenko, Y. Bezkorovainyi, et al., Efficiency analysis of current repair procedures for aviation radio equipment, in: I. Ostroumov, M. Zaliskyi (Eds.), *Proceedings of the 2nd International Workshop on Advances in Civil Aviation Systems Development. ACASD 2024. Lecture Notes in Networks and Systems*, vol. 992, Springer Nature Switzerland, Cham, 2024, pp. 281–295. doi:10.1007/978-3-031-60196-5_21.
- [15] O. Sushchenko, A. Goncharenko, Design of robust systems for stabilization of unmanned aerial vehicle equipment, *International Journal of Aerospace Engineering* (2016) 1–10. doi:10.1155/2016/6054081.
- [16] T. Nikitina, B. Kuznetsov, Y. Averyanova, O. Sushchenko, I. Ostroumov, N. Kuzmenko, et al., Method for design of magnetic field active silencing system based on robust meta model, in: S. Shukla, H. Sayama, J. V. Kureethara, D. K. Mishra (Eds.), *Data Science and Security. IDSCS 2023. Lecture Notes in Networks and Systems*, vol. 922, Springer Nature Singapore, Singapore, 2024, pp. 103–111. doi:10.1007/978-981-97-0975-5_9.
- [17] O. Sushchenko, Y. Bezkorovainyi, O. Solomentsev, M. Zaliskyi, O. Holubnychyi, I. Ostroumov, et al., Algorithm of determining errors of gimbaled inertial navigation system, in: O. Gervasi, B. Murgante, C. Garau, D. Taniar, A. M. A. C. Rocha, M. N. Faginas Lago (Eds.), *Computational Science and Its Applications – ICCSA 2024 Workshops. ICCSA 2024. Lecture Notes in Computer Science*, vol. 14816, Springer Nature Switzerland, Cham, 2024, pp. 206–218. doi:10.1007/978-3-031-65223-3_14.
- [18] O. Ivashchuk, et al., A configuration analysis of ukrainian flight routes network, in: *2021 IEEE 16th International Conference on the Experience of Designing and Application of CAD Systems (CADSM)*, 2021, pp. 6–10. doi:10.1109/CADSM52681.2021.9385263.
- [19] B. Chanetz, J. Déleroy, P. Gilliéron, E. R. Gnemmi, P. Gowree, P. Perrier, *Experimental Aerodynamics*, Springer, Cham, 2022.
- [20] C. D. Britcher, D. Landman, *Wind Tunnel Test Technique*, Academic Press, Cambridge, 2024.
- [21] J. B. Barlow, W. H. Rat, *Low-Speed Wind Tunnel Testing*, John Wiley & Sons, London, 1999.
- [22] D. Sundararajan, *Digital Signal Processing: An Introduction*, Springer, Cham, 2024.
- [23] J. R. Taylor, *An Introduction to Error Analysis: The Study of Uncertainties in Physical Measurements*, Mill Valley, California, 2022.
- [24] J. P. Buonaccorsi, *Measurement Error: Models, Methods and Applications*, CRC Press, Boca Raton,

2010.

- [25] R. Jennings, A. D. L. Cueva, *LabVIEW Graphical Programming*, McGraw-Hill, 2019.
- [26] R. B. Larsen, *LabVIEW for Engineers*, Pearson, London, 2010.
- [27] B. Ehsayi, *Data Acquisition Using LabVIEW*, Packt Publishing, Birmingham, 2016.
- [28] V. Chikovani, O. Sushchenko, H. Tsiruk, Redundant information processing techniques comparison for differential vibratory gyroscope, *Eastern-European Journal of Enterprise Technologies* 4 (2016) 45–52. doi:10.15587/1729-4061.2016.75206.
- [29] O. A. Sushchenko, Y. M. Bezkorovainyi, V. O. Golitsyn, Fault-tolerant inertial measuring instrument with neural network, in: *Proceedings of IEEE 40th International Conference on Electronics and Nanotechnology*, Kyiv, Ukraine, 2020, pp. 797–801. doi:10.1109/ELNANO50318.2020.9088779.
- [30] R. S. Voliansky, A. V. Sadovoi, The transformation of linear dynamical object's equation to brunovsky canonical form, in: *Proceedings of IEEE 4th International Conference Actual Problems of Unmanned Aerial Vehicles Developments*, Kyiv, Ukraine, 2017, pp. 196–199. doi:10.1109/APUAVD.2017.8308808.
- [31] B. I. Kuznetsov, T. B. Nikitina, I. V. Bovdui, Structural-parametric synthesis of rolling mills multi-motor electric drives, *Electrical Engineering & Electromechanics* (2020) 25–30. doi:10.20998/2074-272X.2020.5.04.
- [32] B. I. Kuznetsov, T. B. Nikitina, I. V. Bovdui, Multiobjective synthesis of two degrees of freedom nonlinear robust control by discrete continuous plant, *Technical Electrodynamics* (2020) 10–14. doi:10.20998/2074-272X.2020.5.04.
- [33] S. Osadchyi, V. Zozulia, Synthesis of optimal multivariable robust systems of stochastic stabilization of moving objects, in: *Proceedings of 5th International Conference Actual Problems of Unmanned Aerial Vehicles Developments*, Kyiv, Ukraine, 2019, pp. 106–111. doi:10.1109/APUAVD47061.2019.8943861.
- [34] S. I. Osadchy, V. A. Zozulya, I. A. Bereziuk, M. M. Melnichenko, Stabilization of the angular position of hexapod platform on board of a ship in the conditions of motions, *Automatic Control and Computer Sciences* 56 (2022) 221–229. doi:10.3103/S0146411622030051.
- [35] K. Dergachov, et al., Gps usage analysis for angular orientation practical tasks solving, in: *Proceedings of 2022 IEEE 9th International Conference on Problems of Infocommunications, Science and Technology*, Kharkiv, Ukraine, 2022, pp. 187–192. doi:10.1109/PICST57299.2022.10238629.
- [36] T. Nikitina, B. Kuznetsov, N. Ruzhentsev, O. Havrylenko, K. Dergachov, V. Volosyuk, et al., Algorithm of robust control for multi-stand rolling mill strip based on stochastic multi-swarm multi-agent optimization, in: S. Shukla, H. Sayama, J. V. Kureethara, D. K. Mishra (Eds.), *Data Science and Security. IDSCS 2023. Lecture Notes in Networks and Systems*, vol. 922, Springer Nature Singapore, Singapore, 2024, pp. 247–255. doi:10.1007/978-981-97-0975-5_22.
- [37] A. Popov, E. Tserne, V. Volosyuk, S. Zhyla, V. Pavlikov, N. Ruzhentsev, et al., Invariant polarization signatures for recognition of hydrometeors by airborne weather radars, in: O. Gervasi, B. Murgante, D. Taniar, B. O. Apduhan, A. C. Braga, C. Garau, A. Stratigea (Eds.), *Computational Science and Its Applications – ICCSA 2023. ICCSA 2023. Lecture Notes in Computer Science*, vol. 13956, Springer Nature Switzerland, Cham, 2023, pp. 201–217. doi:10.1007/978-3-031-36805-9_14.